

Separating and transporting of particles using tightly focused radially polarized Bessel–Gaussian beam with conical phase

CHENXU LU, JINSONG LI*, HAORAN ZHANG

China Jiliang University, College of Optics and Electronic, Hangzhou 310018, P.R. China

*Corresponding author: lijinsong@cjlu.edu.cn

The intensity distributions near the focus for radially polarized Bessel–Gaussian beam with conical phase by a high numerical aperture objective are computed based on the vector diffraction theory. Results show that the circular focal spot can be changed from one to two on the focal plane by adjusting the truncation parameter β . By increasing the phase modulation parameter L , the focal pattern appeared focal shift. According to the intensity distribution, the forces acting on a particle are calculated. The stability of particle trapping is analyzed. It is shown that a tightly focused radially polarized Bessel–Gaussian beam with conical phase is applicable to trapping, separating and transporting of particles.

Keywords: conical phase, particle separation, particle transport, Bessel–Gaussian beam.

1. Introduction

Since ASHKIN *et al.* demonstrated that a single focused laser beam can trap dielectric microspheres at the focal point in 1986 [1], optical traps and manipulations [2] have attracted much attention from scholars because they have become important tools for manipulating a variety of particles, including neutral atoms and molecules [3,4], miniature dielectric particles [5-9], DNA molecules [10,11], viruses [12], and living biological cells [13-17]. As far as we know, light has momentum and energy, and the light radiant force is generated by the exchange of energy and momentum between photons and particles. Because elementary Gaussian beams have peaks in the intensity distribution, generally most optical traps and manipulations use focused elementary Gaussian beams. By now, a variety of laser beams with Gaussian-like intensity profile have been studied to trap particles. For example, LIU and ZHAO numerically investigated the trapping effect of the focused generalized Multi-Gaussian Schell model beam at the focal plane [18]. NIE *et al.* compared the focusing properties of the radially polarized Laguerre–Bessel–Gaussian beams with those of Laguerre–Gaussian and Bessel

–Gaussian modes and further analyzed the highly focused radially polarized Laguerre–Bessel–Gaussian beams which can capture two Rayleigh particles stably [19]. DUAN *et al.* [20] derived analytical expressions for the intensity and radiation forces of a focused partially coherent modified Bessel–Gaussian (MBG), and used them to study the optical trapping effect of the focused partially coherent MBG beams acting on dielectric sphere with different refractive indices [20]. It is shown that laser beams with Gaussian-like intensity profile should be used to trap particles with refractive index bigger than that of the ambient, while laser beams with a hollow-like intensity profile are applicable to trap particles with refractive index smaller than the ambient. In addition, it is noted that some other beams such as Hermite–Gaussian beam [21,22], on-axis circularly symmetric Bessel beam [23], Laguerre–Gaussian beam [24], radially polarized beam [25,26], vortex beam [27–29], and circular Airy beams [30] also have been explored. These beams have great application prospects in free space information transmission and optical communication [31–33], optical imaging [34] and optical manipulation [35–37]. However, as far as we know, separating and transporting particles of tightly focused radially polarized Bessel–Gaussian beam with conical phase have not been reported.

In this paper, we investigated the intensity distribution in the focal plane formed by a radially polarized Bessel–Gaussian beam with conical phase. By comparing the forces exerted on the particles under different values of the truncation parameter β and the phase modulation parameter L , some interesting and useful results are found.

2. Theory

In the focusing system, the incident beam is the radially polarized Bessel–Gaussian beam and the phase mask with conical phase distribution is placed in front of the aperture plane of the lens; then the modulated beam with conical phase distribution is focused through an objective lens. Assuming that the radius of the optical aperture is a , the transmittance function of the phase mask can be written as

$$\rho(r, \varphi) = \begin{cases} \exp(-i\varphi), & r < a \\ 0, & \text{otherwise} \end{cases} \quad (1)$$

where r and φ are the cylindrical coordinates, and phase variation in a circular phase mask with conical phase distribution can be written as

$$\varphi = 2\pi L \left(K - \frac{r}{a} \right) \quad (2)$$

where K is between 0 and 1, and L denotes the phase modulation parameters. The Bessel–Gaussian beam with conical phase wavefront is focused. $I(\theta)$ is the amplitude distribution of the incident beam, which can be written as

$$l(\theta) = J_1\left(\frac{2\beta \sin \theta}{\sin \alpha}\right) \exp\left(-\frac{\beta^2 \sin^2 \theta}{\sin^2 \alpha}\right) \exp(-i\varphi) \quad (3)$$

where J_1 denotes the Bessel function of first order, β denotes the truncation parameter, and $\alpha = \arcsin(\text{NA}/n)$ is the maximum of the convergence angle θ . NA is the numerical aperture of the focusing system. According to the vector diffraction theory [38], the electric field $E(r, z)$ and magnetic field $H(r, z)$ near the focus can be written as

$$E_r(r, z) = A \int_0^\alpha \sqrt{\cos \theta} \sin(2\theta) l(\theta) J_1(kr \sin \theta) \exp(ikz \cos \theta) d\theta \quad (4)$$

$$E_z(r, z) = 2iA \int_0^\alpha \sqrt{\cos \theta} \sin(2\theta) l(\theta) J_0(kr \sin \theta) \exp(ikz \cos \theta) d\theta \quad (5)$$

$$H_\varphi(r, z) = \frac{2An}{\mu_0 c} \int_0^\alpha \sqrt{\cos \theta} \sin(\theta) l(\theta) J_1(kr \sin \theta) \exp(ikz \cos \theta) d\theta \quad (6)$$

where r and z are the cylindrical coordinates, respectively. In Eqs. (4)–(6), α is the convergence angle of the objective, $A = E\pi f n^{1/2}/\lambda$, E is the amplitude of electric field in a vacuum, which is related to the power of the incident beam, f is the focal length of the lens, $k = 2\pi n/\lambda$ is the wave number in the immersion liquid with the refractive index n , J_n is the n -th-order Bessel function of the first kind.

The total light intensity in the focusing region can be written as

$$I(r, z) = |E_r(r, z)|^2 + |E_z(r, z)|^2 \quad (7)$$

The average Poynting vector can be written as

$$\langle S \rangle = \frac{1}{2} \left\{ \text{Re} \left[E_r(r, z) H_\varphi^*(r, z) \right] \mathbf{e}_z - \text{Re} \left[E_z(r, z) H_\varphi^*(r, z) \right] \mathbf{e}_r \right\} \quad (8)$$

where \mathbf{e}_r is the unit vectors in the radial direction, and \mathbf{e}_z is the unit vectors in the longitudinal direction.

In a light field, a Rayleigh particle can be considered a point dipole because its radius is much smaller than the incident wavelength. The polarizability of a point dipole can be expressed as follows

$$\alpha = 4a^3 \varepsilon_1 \frac{\varepsilon_2 - \varepsilon_1}{\varepsilon_2 + \varepsilon_1} \quad (9)$$

where a represents the radius of the Rayleigh particle, ε_1 is the dielectric constants of the particle, and ε_2 is the dielectric constants of the medium surrounding the particle.

Based on Rayleigh scattering theory [25], the gradient, absorption and scattering forces can be written as

$$F_{\text{grad}} = \frac{1}{4} \operatorname{Re}(\alpha) \varepsilon_0 \nabla I(r, z) \quad (10)$$

$$F_{\text{abs}} = \frac{n \langle S \rangle C_{\text{abs}}}{c} \quad (11)$$

$$F_{\text{scat}} = \frac{n \langle S \rangle C_{\text{scat}}}{c} \quad (12)$$

where ε_0 is the permittivity in a vacuum, $C_{\text{scat}} = k^4 |\alpha|^2 / 6\pi$ and $C_{\text{abs}} = kn \operatorname{Im}(\alpha) / \varepsilon_1$ is the absorption and scattering cross-sections, respectively. Re and Im represent real and imaginary parts, respectively.

3. Numerical results

In this section, the focusing properties of tightly focused radially polarized Bessel–Gaussian beam with conical phase under different truncation parameter β and phase modulation parameters L is examined. In the numerical simulation, the refraction index $n = 1.332$, the numerical aperture $\text{NA} = 0.95n$, the incident wavelength $\lambda = 1047 \text{ nm}$.

In order to investigate the effect of β on the intensity distribution of the beam, the intensity of Bessel–Gaussian beam with conical phase at the conditions of $L = 1$ is illustrated and analyzed in Fig. 1. We can see that the distribution of light intensity

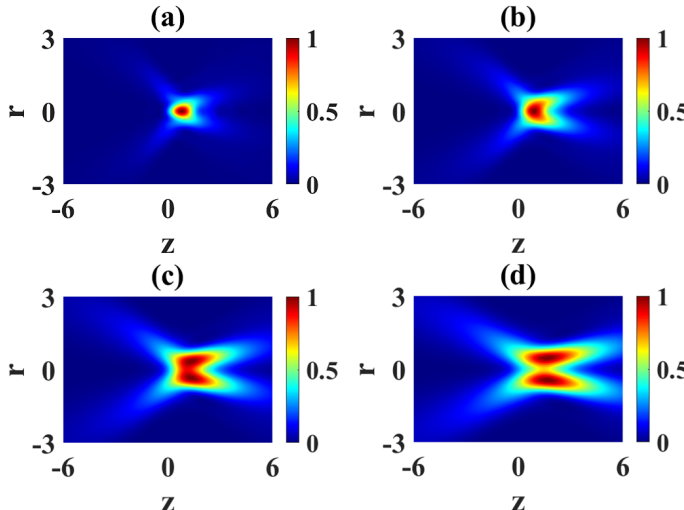


Fig. 1. Focusing field intensity distributions of Bessel–Gaussian beam with conical phase wavefront under condition of $L = 1$ and (a) $\beta = 1.3$, (b) $\beta = 1.6$, (c) $\beta = 1.9$, and (d) $\beta = 2.2$, respectively.

changes considerably with the truncation parameter β . It can be seen that with β increases, the focus pattern of the optical intensity slowly enlarges and starts to split along the radial direction until it splits into two. Comparing Figs. 1(a) and (d), a small focal pattern becomes two large ones. Figure 1 shows the truncation parameter β has a great influence on the optical intensity distribution in the focal region, and the focal pattern is wholly enlarged and splits in two at the focal plane. The results show that β value can effectively adjust the number of the focal pattern to achieve the purpose of particle separation.

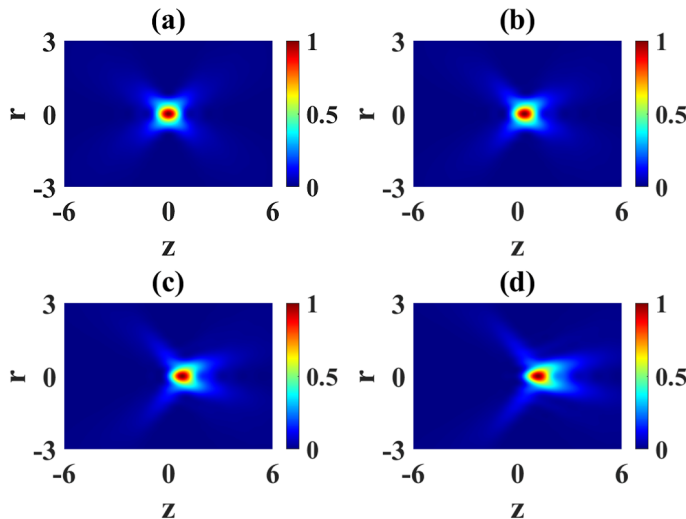


Fig. 2. Focusing field intensity distributions of Bessel–Gaussian beam with conical phase wavefront under condition of $\beta = 1.3$ and (a) $L = 0$, (b) $L = 0.5$, (c) $L = 1$, and (d) $L = 1.5$.

Aiming at exploring the effect of different phase modulation parameters on the intensity distribution of the focusing plane, we simulated the focused intensity distribution of the Bessel–Gaussian beam with conical phase wavefront at $\beta = 1.3$, as shown in Fig. 2. Under the condition of phase modulation parameter $L = 0$, it shows a focal pattern is at the center of the focal plane. As L increases, the focal pattern of light intensity is shifted along the positive direction of the z -axis. It can be said that the focal pattern can be adjusted horizontally along the positive direction of the z -axis by introducing the conical phase, and the larger L is, the greater moving distance of the focal pattern. The results show that L value can effectively adjust the position of the focal pattern to achieve the purpose of particle transport.

Figure 3 illustrates the evolution of intensity distributions in the focal region for $\beta = 2$ with changing the phase modulation parameters L , which shows that the intensity distribution in the focal region can be altered considerably by the phase modulation parameters L . The total light intensity distribution in the focal plane has two intensity peaks, which are symmetrically distributed along the r -axis, as shown in Fig. 3(a). Similarly, when L increases to 1.5, the focal pattern of light intensity is shifted along the

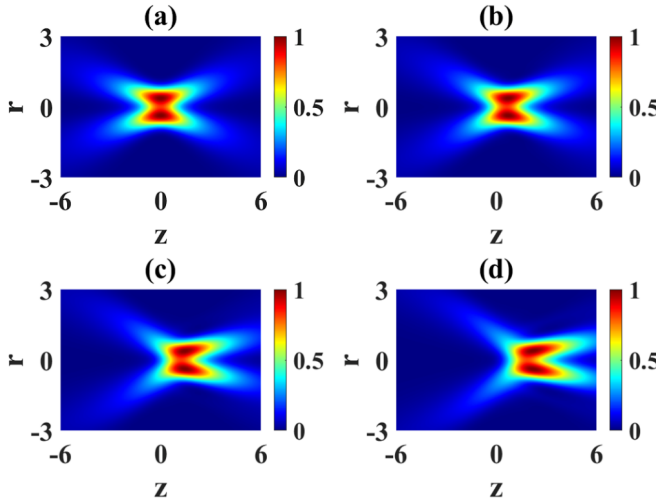


Fig. 3. Focusing field intensity distributions of Bessel–Gaussian beam with conical phase wavefront under condition of $\beta = 2$ and (a) $L = 0$, (b) $L = 0.5$, (c) $L = 1$, and (d) $L = 1.5$.

positive direction of the z -axis. The results show that L value can effectively adjust the position of the focal pattern to achieve the purpose of particle transport.

This focusing field variation feature is of unusual consequence for the extended study of Bessel–Gaussian beam in biological imaging, optical focusing and other fields. Comparing Figs. 2 and 3, although the shapes of the focal patterns are different, they move in the same way with larger L . Then, we numerically calculate the forces acting on the particle in order to further analyze the feasibility of particle separation and particle transport. In the numerical calculation, we take a particle with a radius of 19.1 nm and relative permittivity $\epsilon = -54 + 5.9i$ as an example to analyze the forces of the beam on the particle.

When gravity and Brownian force are small enough, as long as the gradient force F_{grad} is larger than the combined force of $F_{\text{abs}} + F_{\text{scat}}$, a stable trap can be achieved at the capture point. We plot intensity distributions of the gradient force F_{grad} and the sum of the absorption and scattering forces $F_{\text{abs}} + F_{\text{scat}}$ acting on a particle for the tightly focused radially polarized Bessel–Gaussian beam under different L along the r and z directions in Fig. 4. From Fig. 4(a)–(d), it can be seen that there is an equilibrium position for trapping particles in both the r and z directions under different L , which means that this type of particle can be transported by adjusting L (see black and red lines). In Fig. 4(a)–(d) and Fig. 4(e)–(h), it can be clearly seen that with the increase of L , the gradient force F_{grad} in the r direction, the sum of the absorption force and the scattering force $F_{\text{abs}} + F_{\text{scat}}$ decreases, but the force in the z direction changes a little. It is clear that the sum of the absorption and scattering forces provides a reduction of factors of two orders of magnitude corresponding to the gradient force. In particular, it should be noted that the scattering or absorption force is essentially null along the beam axis, which is consistent with that in [25, 39].

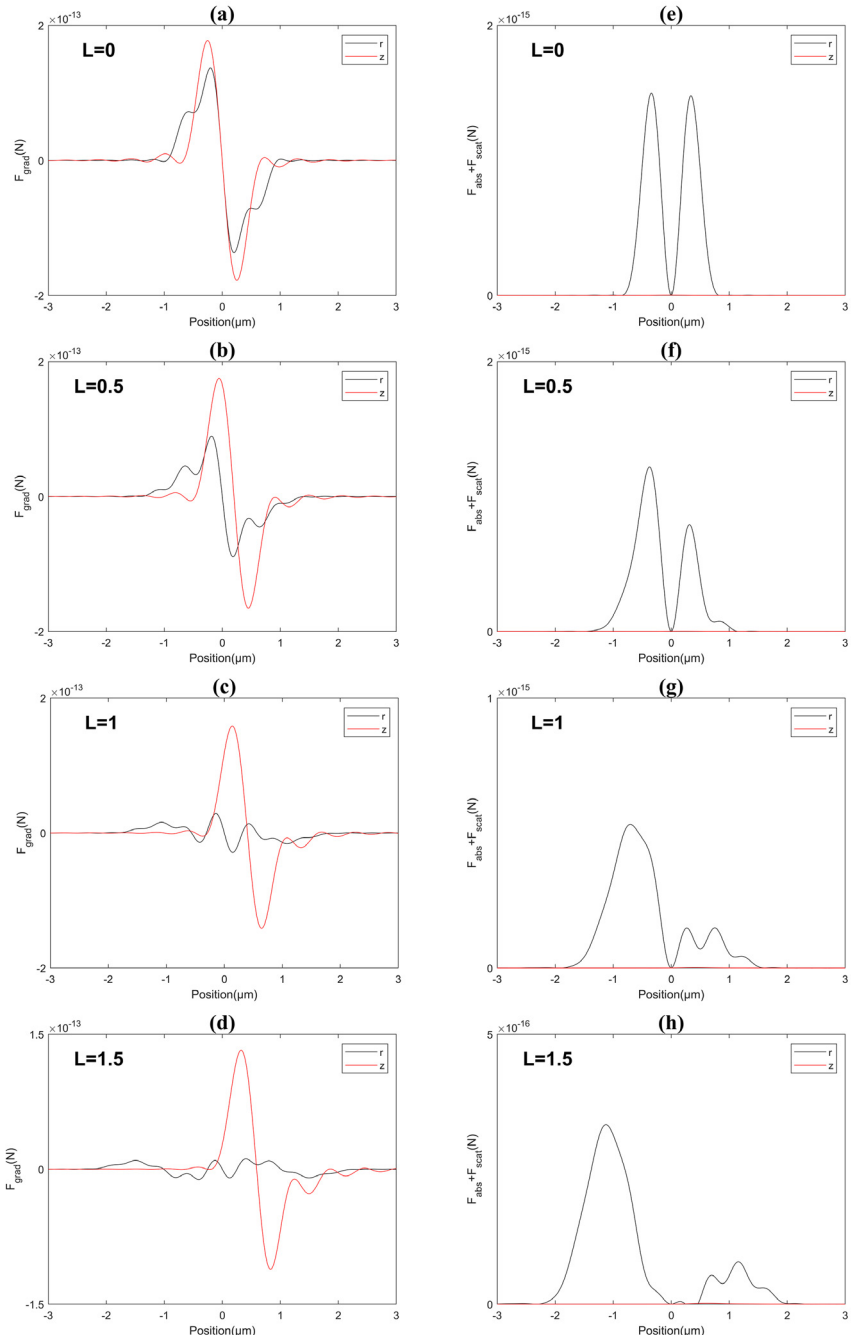


Fig. 4. Forces of Bessel-Gaussian beam with conical phase ($\beta = 1.3$) acting on a particle. The gradient force of (a) $L = 0$, (c) $L = 0.5$, (e) $L = 1$, (g) $L = 1.5$, the sum of the absorption force and scattering force of (b) $L = 0$, (d) $L = 0.5$, (f) $L = 1$, (h) $L = 1.5$ along the r direction and z direction in the focal plane. The radius of the particle is 19.1 nm, and the relative permittivity is $\epsilon = -54 + 5.9i$.

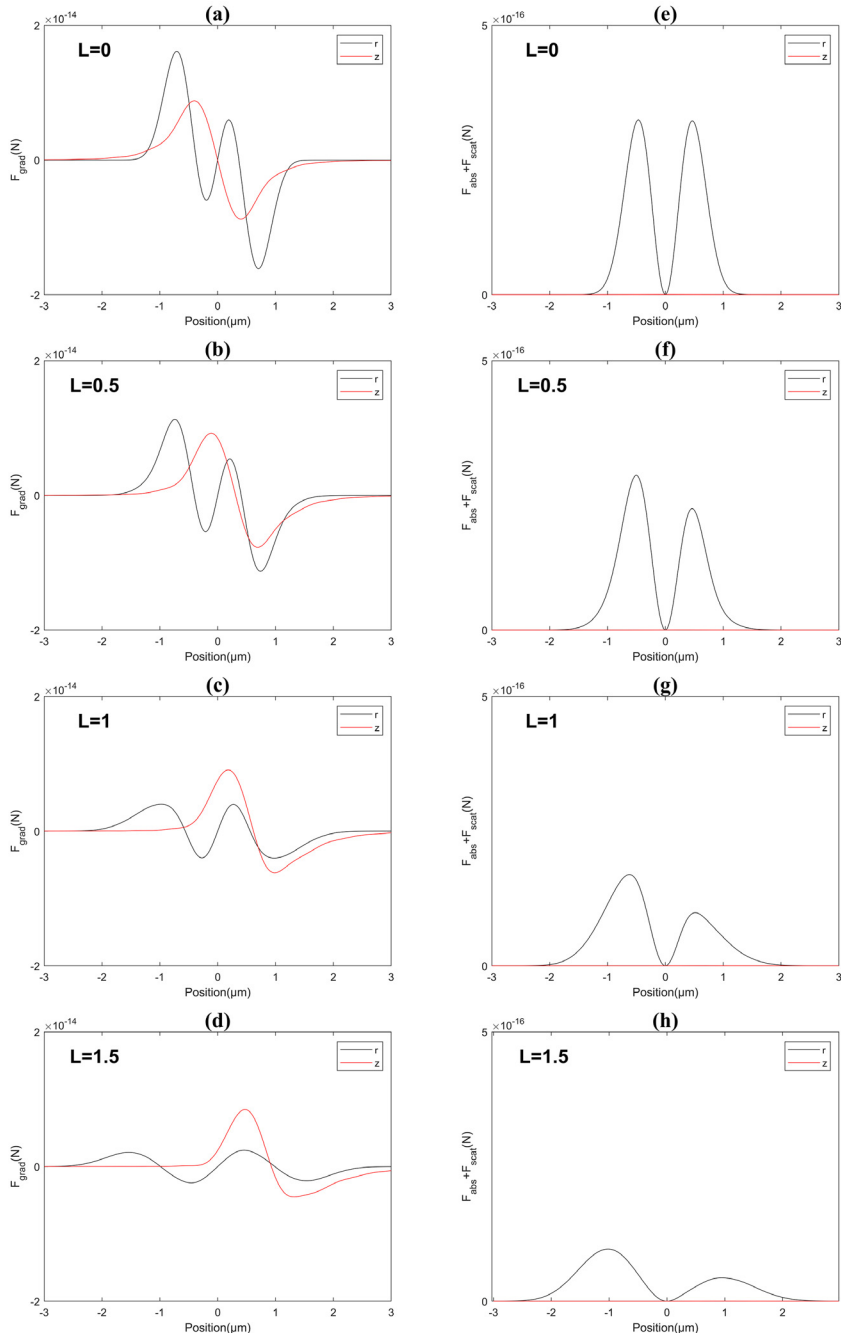


Fig. 5. Forces of Bessel-Gaussian beam with conical phase ($\beta = 2$) acting on a particle. The gradient force of (a) $L = 0$, (c) $L = 0.5$, (e) $L = 1$, (g) $L = 1.5$, the sum of the absorption force and scattering force of (b) $L = 0$, (d) $L = 0.5$, (f) $L = 1$, (h) $L = 1.5$ along the r direction and z direction the focal plane. The radius of the particle is 19.1 nm, and the relative permittivity is $\epsilon = -54 + 5.9i$.

Now we turn to the case of the truncation parameter $\beta = 2$. In Fig. 5(a)–(d), there exist two equilibrium points along the r direction, which means that such particles will be separated by the focused radially Bessel–Gaussian polarized beams. However, in contrast to Fig. 4(a)–(d), the optical cage gives rise to smaller gradient force as seen in Fig. 5(a)–(d). Similarly, the calculation shows that there is no energy flow along the beam axis and the forces in other directions all decrease with the increase of L . Meanwhile, the sum of the scattering and absorption forces in the two directions is much smaller than the corresponding gradient forces.

Then we calculate two stability criteria for manipulating particles by using tightly focused radially polarized Bessel–Gaussian beam with conical phase. On the one hand, all components of the gradient force should be larger than the sum of absorption and scattering forces, *i.e.*, $R = F_{\text{grad}}/(F_{\text{abs}} + F_{\text{scat}}) > 1$, where R is called the stability criterion. For a conservative estimation, we can use $R = (F_{\text{grad}})_{\text{max}}/(F_{\text{abs}} + F_{\text{scat}})_{\text{max}} > 1$ to estimate the stability [25,39]. By using simple computations?in the case of $\beta = 1.3$, when $L = 0$, $R = 91, \infty$ along the r and z directions, respectively; when $L = 0.5$, $R = 73, \infty$ along the r and z directions, respectively; when $L = 1$, $R = 54, \infty$ along the r and z directions, respectively; when $L = 1.5$, $R = 34, \infty$ along the r and z directions, respectively. In the case of $\beta = 2$, when $L = 0$, $R = 50, \infty$ along the r and z directions, respectively; when $L = 0.5$, $R = 39, \infty$ along the r and z directions, respectively; when $L = 1$, $R = 24, \infty$ along the r and z directions, respectively; when $L = 1.5$, $R = 22, \infty$ along the r and z directions, respectively. The results clearly show that particles can be stably trapped, separated and transported by using tightly focused radially polarized Bessel–Gaussian beam with conical phase.

On the other hand, a stable trapping system requires that the potential well generated by the gradient forces should be sufficiently deep to overcome the kinetic energy of the trapping particle in Brownian motion. A widely used criterion for particle trapping stability is known as the Boltzmann factor, as follows

$$R_{\text{thermal}} = \exp\left(-\frac{U_m}{k_B T}\right) \leq 1 \quad (13)$$

where k_B is the Boltzmann constant, T is the temperature of the ambient, and U_m is the maximum depth of the potential well expressed as $|R_e(\alpha)\varepsilon_0 I(r, z)_{\text{max}}/2|$. Assuming temperature 300 K, R_{thermal} for the situations considered in Fig. 2(a)–(d) is calculated to be 1.32×10^{-15} , 1.38×10^{-15} , 4.74×10^{-14} and 2.02×10^{-12} . The R_{thermal} for the situations considered in Fig. 3(a)–(d) is calculated to be 0.018, 0.019, 0.022 and 0.029, respectively. The above results show that particles can be stably trapped, separated and transported by using tightly focused radially polarized Bessel–Gaussian beam with conical phase. These results have academic significance and the optical field distribution in the focus region is complicated, which makes it possible to carry more information in the optical information transmission field.

4. Conclusions

In conclusion, we investigated the intensity distribution in the focal plane formed by a tightly focused radially polarized Bessel–Gaussian beam with conical phase. The effects of the truncation parameter β and the phase modulation parameter L on the normalized intensity distribution are discussed in detail. The results show that the focal pattern can be changed from one to two on the focal plane by adjusting the truncation parameter β . The phase modulation parameter L can significantly adjust the position of the intensity peak, by increasing L , the position of the maximum intensity spot will move along the z -axis. According to the intensity distribution, the forces acting on a particle are calculated. In addition, it is indicated that the optical trap is stable. This unique focusing patterns are difficult to be obtained with other types of light beams, however, it has been achieved by using the proposed Bessel–Gaussian beam. This work not only deduces the optical field distribution in the focusing area of the radially polarized Bessel–Gaussian beam with conical phase which provides a reference value for related research, but also expands the potential application prospect of particle trapping, particle separation and particle transport.

References

- [1] ASHKIN A., DZIEDZIC J.M., BJORKHOLM J.E., *Observation of a single-beam gradient force optical trap for dielectric particles*, Optics Letters **11**, 1986: 288-290.
- [2] YAVUZ D.D., KULATUNGA P.B., URBAN E., *Fast ground state manipulation of neutral atoms in microscopic optical traps*, Physical Review Letters **96**, 2006: 063001.
- [3] ASHKIN A., *Trapping of atoms by resonance radiation pressure*, Physical Review Letters **40**, 1978: 729-732.
- [4] ZHANG P., LI G., ZHANG T., *Subwavelength optical dipole trap for neutral atoms using a micro-capillary tube tip*, Journal of Physics B **50**, 2017: 045005.
- [5] CALANDER N., WILLANDER M., *Optical trapping of single fluorescent molecules at the detection spots of nanoprobes*, Physical Review Letters **89**, 2002: 143603.
- [6] BAUMGARTL J., MAZILU M., DHOLAKIA K., *Optically mediated particle clearing using Airy wavepackets*, Nature Photonics **2**, 2008: 675-678.
- [7] GU B., PAN Y., RUI G., *Polarization evolution characteristics of focused hybridly polarized vector fields*, Applied Physics B **117**, 2014: 915-926.
- [8] HE H., FRIESE M.E.J., HECKENBERG N.R., *Direct observation of transfer of angular momentum to absorptive particles from a laser beam with a phase singularity*, Physical Review Letters **75**, 1995: 826-829.
- [9] NOVITSKY A., QIU C.W., WANG H., *Single gradientless light beam drags particles as tractor beams*, Physical Review Letters **107**, 2011: 203601.
- [10] TSKHOVREBOVA L., TRINICK J., SLEEP J.A., *Elasticity and unfolding of single molecules of the giant muscle protein titin*, Nature **387**, 1997: 308-312.
- [11] WANG M.D., YIN H., LANDICK R., *Block SM. Stretching DNA with optical tweezers*, Biophysical Journal **72**, 1997: 1335-1346.
- [12] PANG Y., SONG H., KIM J.H., *Optical trapping of individual human immunodeficiency viruses in culture fluid reveals heterogeneity with single-molecule resolution*, Nature Nanotechnology **9**, 2014: 624-630.

- [13] BLOCK S.M., GOLDSTEIN L.S.B., SCHNAPP B.J., *Bead movement by single kinesin molecules studied with optical tweezers*, Nature **348**, 1990: 348-352.
- [14] TSKHOVREBOVA L., TRINICK J., SLEEP J.A., *Elasticity and unfolding of single molecules of the giant muscle protein titin*, Nature **387**, 1997: 308-312.
- [15] ZHONG M.C., WEI X.B., ZHOU J.H., *Trapping red blood cells in living animals using optical tweezers*, Nature Communications **4**, 2013: 1768.
- [16] LIU R., ZHENG L., MATTHEWS D.L., *Power dependent oxygenation state transition of red blood cells in a single beam optical trap*, Applied Physics Letters **99**, 2011: 043702.
- [17] LIU R., MAO Z., MATTHEWS D.L., *Novel single-cell functional analysis of red blood cells using laser tweezers Raman spectroscopy: Application for sickle cell disease*, Experimental Hematology **41**, 2013: 656-661.
- [18] LIU X., ZHAO D., *Trapping two types of particles with a focused generalized multi-Gaussian Schell model beam*, Optics Communications **354**, 2015: 250-255.
- [19] NIE Z., SHI G., LI D., *Tight focusing of a radially polarized Laguerre-Bessel-Gaussian beam and its application to manipulation of two types of particles*, Physics Letters A **379**, 2015: 857-863.
- [20] DUAN M., ZHANG H., LI J., *Trapping two types of particles using a focused partially coherent modified Bessel-Gaussian beam*, Optics and Lasers in Engineering **110**, 2018: 308-314.
- [21] SU J., NAN N., MOU J., *Simultaneous trapping of two types of particles with focused elegant third-order Hermite-Gaussian beams*, Micromachines **12**, 2020: 769.
- [22] XU Z., LIU X., CHEN Y., *Self-healing properties of Hermite-Gaussian correlated Schell-model beams*, Optics Express **28**, 2020: 2828.
- [23] GOUESBET G., AMBROSIO L., *Rayleigh limit of generalized Lorenz-Mie theory for on-axis beams and its relationship with the dipole theory of forces. Part I: Non dark axisymmetric beams of the first kind, with the example of Gaussian beams*, Journal of Quantitative Spectroscopy and Radiative Transfer **266**, 2021: 107569.
- [24] HERNE C.M., CAPUZZI K.M., SOBEL E., *Rotation of large asymmetrical absorbing objects by Laguerre-Gauss beams*, Optics Letters **40**, 2015: 4026-4029.
- [25] ZHANG Y., DING B., SUYAMA T., *Trapping two types of particles using a double-ring-shaped radially polarized beam*, Physical Review A **81**, 2010: 023831.
- [26] ZHUANG Y., ZHANG Y., DING B., *Trapping Rayleigh particles using highly focused higher-order radially polarized beams*, Optics Communications **284**, 2011: 1734-1739.
- [27] CHEN M., WU P., ZENG Y., *Trapping dielectric Rayleigh particles with tightly focused pin-like vortex beam*, European Physical Journal D **76**, 2022: 20.
- [28] WANG Q., ZHANG L., KE L., *Parameters controlling of vortex solitons in nonlocal nonlinear medium with gradually characteristic length*, Chaos, Solitons & Fractals **161**, 2022: 112319.
- [29] FAN C., XANG Y., CHEN Z., *Trapping two types of particles by using a tightly focused radially polarized power-exponent-phase vortex beam*, Journal of the Optical Society of America A **35**, 2018: 903-907.
- [30] JIANG Y., CAO Z., SHAO H., *Trapping two types of particles by modified circular Airy beams*, Optics Express **24**, 2016: 18072-18081.
- [31] ZHANG X., XIA T., CHENG S., *Free-space information transfer using the elliptic vortex beam with fractional topological charge*, Optics Communications **431**, 2018: 238-244.
- [32] SHAO W., HUANG S., LIU X., *Free-space optical communication with perfect optical vortex beams multiplexing*, Optics Communications **427**, 2018: 545-550.
- [33] WANG J., YANG J., FAZAL I.M., *Terabit free-space data transmission employing orbital angular momentum multiplexing*, Nature Photonics **6**, 2012: 488-496.
- [34] MAURER C., JESACHER A., BERNET S., *What spatial light modulators can do for optical microscopy*, Laser & Photonics Reviews **5**, 2011, 81-101.
- [35] PENG J., JIA S., ZHANG C., *Optical force and torque on small particles induced by polarization singularities*, Optics Express **30**, 2022: 16489-16498.

- [36] WU Y., WU J., LIN Z., *Propagation properties and radiation forces of the Hermite-Gaussian vortex beam in a medium with a parabolic refractive index*, Applied Optics **59**, 2020: 8342.
- [37] FORBES K., GREEN D., *Enantioselective optical gradient forces using 3D structured vortex light*, Optics Communications **515**, 2022: 128197.
- [38] WOLF E., *Electromagnetic diffraction in optical systems. I. An integral representation of the image field*, Proceedings of the Royal Society of London **253**, 1959: 349-357.
- [39] ZHAN Q., *Trapping metallic Rayleigh particles with radial polarization*, Optics Express **12**, 2004: 3377-3382.

*Received December 30, 2022
in revised form March 3, 2023*